ICA 2022
24th INTERNATIONAL CONGRESS ON ACOUSTICS
October 24(Mon) - 28(Fri), 2022 Gyeongju, Korea

PROCEEDINGS of the
24th International Congress on Acoustics

October 24 to 28, 2022 in Gyeongju, Korea

Audio sound field generated by a parametric array loudspeaker in a rectangular room with lightly damped walls

Jiaxin ZHONG[(1)], Ray KIRBY[(1)], Mahmoud KARIMI[(1)], Xiaojun QIU[(2)], Jing LU[(2)]

[(1)]Centre for Audio, Acoustics, and Vibration, University of Technology Sydney, New South Wales 2007, Australia

[(2)]Key Laboratory of Modern Acoustics and Institute of Acoustics, Nanjing University, Nanjing 210093, China

ABSTRACT

Parametric array loudspeakers (PALs) are known for their ability of generating highly directional sound beams. Existing research focuses on the generated sound field in free field but pays little attention to the wave propagation in a room. This paper aims to investigate the audio sound generated by a PAL in a two-dimensional rectangular room with lightly damped walls. An expression of the audio sound is derived first based on the normal mode analysis and the quasilinear solution of the Westervelt equation. The nonlinear local effects are then included by adding an algebraic correction to the solution. The simulation results are presented and compared to the audio sound field generated by a PAL in free field. Unlike the PAL in free field, it is found that the local effects cannot be neglected when the PAL is placed in a room. It is also observed that the audio beam still focuses along the radiation axis of the PAL in a room albeit there are fluctuations in the propagating direction.

Keywords: Parametric array loudspeaker, Directional sound beams, Modal analysis, Room acoustics

1 INTRODUCTION

Parametric array loudspeakers (PALs) have been widely used in many audio applications due to their ability of generating highly directional audio beams at low frequencies (1). In recent years, their applications have been explored in areas such as active noise control (2) and multi-beam design (3, 4). When a PAL generates two intensive ultrasonic beams at two different frequencies, the audio sound at the difference frequency is demodulated due to the nonlinear interaction between the beams. Extensive literatures have been published to investigate the propagation of sound waves generated by a PAL in free field (5, 6). The audio sound field generated by a PAL in free field is quite different from that generated by a conventional dynamic loudspeaker due to the nonlinear nature of PALs (6). PALs might be used in a room (7), yet little publication was found concerning on modelling sound generated by a PAL in a room. This will be addressed in this paper.

The generation of the audio sound from ultrasonic waves is a complicated process, so that the governing equation is more difficult to solve than that for a linear radiation problem. Because the ultrasound level generated by a PAL is limited due to safety concerns, the nonlinearity is weak and the quasilinear approximation can be assumed to simplify the calculations (1). Under this framework, the audio sound can be considered as the linear radiation from a volume source with its source density proportional to the product of ultrasound pressure (6). Based on the quasilinear solution, many numerical models have been proposed to predict the audio sound in free field, such as the Gaussian beam expansion (8), the spherical wave expansion (9), and the convolution model (10). For the sound propagation in a room, the modal analysis was a classical model to obtain the sound field (11). However, it has not been used to model the sound generated by a PAL in a room.

In this paper, the quasilinear solution based on the Westervelt equation is presented first. An algebraic correction is used to correct the obtained solution to include the local effects which are found to be significant in the near field (12). The ultrasound field in a two-dimensional (2D) rectangular room with lightly damped walls is derived using the normal mode expansion. The audio sound is then obtained by substituting the normal mode expansion into the quasilinear solution. Numerical results are presented and discussed.

2 METHODS

Figure 1 shows the physical model to be investigated in this paper. A PAL is modelled by a line source with a half-width of a, and is placed in a 2D rectangular room with dimensions of $S = L_x \times L_y$. A rectangular coordinate system Oxy is established with its origin at the left corner. The centroid of the PAL is located at $\boldsymbol{\rho}_\mathrm{s} = (x_\mathrm{s}, y_\mathrm{s})$. The radiation direction of the PAL is determined by a vector $\mathbf{n}_\mathrm{s} = (n_{\mathrm{s},x}, n_{\mathrm{s},y})$. For example, the vector $\mathbf{n}_\mathrm{s} = (0,1)$ means the radiation direction is in the positive y axis. The walls are denoted by ∂S and it is assumed that they have a normalized specific acoustic admittance of $\chi(\boldsymbol{\rho})$ at the location $\boldsymbol{\rho} = (x,y)$. The PAL is assumed to generate two ultrasonic waves at frequencies of f_1 and f_2 ($f_1 < f_2$), and the audio sound generated is at the frequency of $f_\mathrm{a} = f_2 - f_1$.

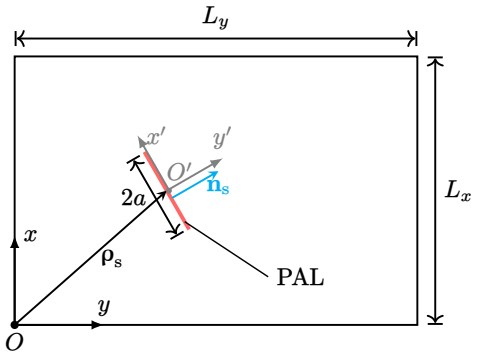

Figure 1. Sketch of a PAL in a 2D rectangular room.

2.1 Quasilinear solution

The radiation of sound from a PAL is governed by the Westervelt equation (5, 6)

$$\nabla^2 p - \frac{1}{c_0^2}\frac{\partial^2 p}{\partial t^2} = -\frac{\delta}{c_0^2}\nabla^2\frac{\partial p}{\partial t} - \frac{\beta}{\rho_0 c_0^4}\frac{\partial^2 p}{\partial t^2} \tag{1}$$

where p is the sound pressure, δ is the sound diffusivity parameter, $\beta = 1.2$ is the nonlinearity coefficient in air, ρ_0 is the air density, c_0 is the sound speed in air, and t is the time.

By using the quasilinear approximation and the successive method, the Westervelt equation can be decomposed into two coupled linear wave equations. Under this framework, the ultrasound field is solved as the linear radiation from an ultrasonic source. The audio sound field is generated by a virtual source with the source density proportional to the product of ultrasound pressure, which reads (5, 6)

$$q_\mathrm{a}(\boldsymbol{\rho}_\mathrm{v}) = \frac{\beta k_\mathrm{a}}{\mathrm{i}\rho_0^2 c_0^3} p_1^*(\boldsymbol{\rho}_\mathrm{v}) p_2(\boldsymbol{\rho}_\mathrm{v}) \tag{2}$$

where i is the imaginary unit, $\boldsymbol{\rho}_\mathrm{v} = (x_\mathrm{v}, y_\mathrm{v})$ are the coordinates of the virtual source point, the superscript "$*$" denotes the complex conjugate, k_a is the wavenumber of audio sound, and $p_i(\boldsymbol{\rho}_\mathrm{v})$ denotes the ultrasound pressure at $\boldsymbol{\rho}_\mathrm{v}$ and frequency of f_i with the ultrasound index $i = 1, 2$. The audio sound pressure at a field point $\boldsymbol{\rho} = (x,y)$ based on the Westervelt equation is obtained as (13)

$$p_\mathrm{a}(\boldsymbol{\rho}) = \frac{\rho_0 c_0 k_\mathrm{a}}{4} \iint_S q(\boldsymbol{\rho}_\mathrm{v}) H_0(k_\mathrm{a}|\boldsymbol{\rho} - \boldsymbol{\rho}_\mathrm{v}|)\mathrm{d}^2\boldsymbol{\rho}_\mathrm{v} \tag{3}$$

where $H_0(\cdot)$ is the first kind Hankel function of order 0. The local effects cannot be captured in Westervelt equation given by Eq. (1), which can be included by adding an algebraic correction to Eq. (3) (12)

$$\tilde{p}_\mathrm{a}(\boldsymbol{\rho}) = p_\mathrm{a}(\boldsymbol{\rho}) - \left[\frac{\rho_0}{2}\mathbf{v}_1^*(\boldsymbol{\rho}) \cdot \mathbf{v}_2(\boldsymbol{\rho}) - \left(\frac{\omega_1}{\omega_2} + \frac{\omega_2}{\omega_1} - 1\right)\frac{p_1^*(\boldsymbol{\rho}) p_2(\boldsymbol{\rho})}{2\rho_0 c_0^2}\right] \tag{4}$$

where $\omega_i = 2\pi f_i$ is the angular frequency, and $\mathbf{v}_i(\boldsymbol{\rho})$ is the particle velocity of ultrasound at the frequency of f_i. It can be obtained by using the linear relation to the ultrasound pressure as

$$\mathbf{v}_i(\boldsymbol{\rho}) = \frac{\nabla p_i(\boldsymbol{\rho})}{\mathrm{i}\rho_0 c_0 k_i}. \tag{5}$$

2.2 Ultrasound field

The ultrasound pressure in a 2D rectangular room with lightly damped walls can be obtained by using the normal mode expansion as (14)

$$p_i(\boldsymbol{\rho}) = \sum_{m_i=0}^{\infty} \frac{\psi_{m_i}(\boldsymbol{\rho}) Q_{m_i}(\boldsymbol{\rho}_\mathrm{s}, \psi)}{\Lambda_{m_i}(k_i^2 - k_{m_i}^2 + \mathrm{i}k_i D_{m_i})} \tag{6}$$

where k_i is the wavenumber at the frequency f_i, the eigenfunctions are

$$\psi_{m_i}(\boldsymbol{\rho}) = \cos\left(k_{m_{i,x}} x\right) \cos\left(k_{m_{i,y}} y\right) \tag{7}$$

with $k_{m_{i,x}} = m_{i,x}\pi/L_x, k_{m_{i,y}} = m_{i,y}\pi/L_y$, m_i denotes the index set of $m_{i,x}$ and $m_{i,y}$, $k_{m_i}^2 = k_{m_{i,x}}^2 + k_{m_{i,y}}^2$

$$\Lambda_{m_i} \equiv \iint_S |\psi_{m_i}(\boldsymbol{\rho})|^2 \mathrm{d}^2\boldsymbol{\rho} = \frac{S}{\varepsilon_{m_i}} \tag{8}$$

$$D_{m_i} \equiv \frac{1}{\Lambda_{m_i}} \int_{\partial S} \chi(\boldsymbol{\rho}') \left|\psi_{m_i}(\boldsymbol{\rho}')\right|^2 \mathrm{d}\boldsymbol{\rho}' \tag{9}$$

$\varepsilon_{m_i} = \varepsilon_{m_{i,x}} \varepsilon_{m_{i,y}}$ is the Neumann factor, the source term is

$$Q_{m_i}(\boldsymbol{\rho}_\mathrm{s}, \psi) = \mathrm{i}\rho_0 c_0 k_i \iint_S q_i(\boldsymbol{\rho}_\mathrm{s}, \boldsymbol{\rho}') \psi_{m_i}(\boldsymbol{\rho}') \mathrm{d}^2\boldsymbol{\rho}' \tag{10}$$

and $q_i(\boldsymbol{\rho}_\mathrm{s}, \boldsymbol{\rho}')$ is the source density at the frequency f_i.

The particle velocity for ultrasound required in Eq. (4) can be obtained by substituting Eq. (6) into Eq. (5)

$$\begin{cases} v_{m_i,x}(\boldsymbol{\rho}) = \dfrac{1}{\mathrm{i}\rho_0 c_0 k_i} \displaystyle\sum_{m_i=0}^{\infty} \frac{-k_{m_{i,x}} \sin\left(k_{m_{i,x}} x\right) \cos\left(k_{m_{i,y}} y\right) Q_{m_i}(\boldsymbol{\rho}_\mathrm{s}, \psi)}{\Lambda_{m_i}(k_i^2 - k_{m_i}^2 + \mathrm{i}k_i D_{m_i})} \\ v_{m_i,y}(\boldsymbol{\rho}) = \dfrac{1}{\mathrm{i}\rho_0 c_0 k_i} \displaystyle\sum_{m_i=0}^{\infty} \frac{-k_{m_{i,y}} \sin\left(k_{m_{i,y}} y\right) \cos\left(k_{m_{i,x}} x\right) Q_{m_i}(\boldsymbol{\rho}_\mathrm{s}, \psi)}{\Lambda_{m_i}(k_i^2 - k_{m_i}^2 + \mathrm{i}k_i D_{m_i})}. \end{cases} \tag{11}$$

For further calculation, it is convenient to rewrite Eq. (6) as

$$p_i(\boldsymbol{\rho}) = \sum_{m_i=-\infty}^{\infty} \frac{\phi_{m_i}(\boldsymbol{\rho}) Q_{m_i}(\boldsymbol{\rho}_\mathrm{s}, \psi)}{S(k_i^2 - k_{m_i}^2 + \mathrm{i}k_i D_{m_i})} \tag{12}$$

where we define the exponential function set

$$\phi_{m_i}(\boldsymbol{\rho}) \equiv \exp\left(\mathrm{i}\mathbf{k}_{m_i} \cdot \boldsymbol{\rho}\right) = \exp\left[\mathrm{i}\left(k_{m_{i,x}} x + k_{m_{i,y}} y\right)\right]. \tag{13}$$

Alternatively, Eq. (6) can be rewritten as

$$p_i(\boldsymbol{\rho}) = \sum_{m_i=-\infty}^{\infty} \frac{\psi_{m_i}(\boldsymbol{\rho}) Q_{m_i}(\boldsymbol{\rho}_\mathrm{s}, \phi)}{S(k_i^2 - k_{m_i}^2 + \mathrm{i}k_i D_{m_i})} \tag{14}$$

where the source term given by Eq. (10) is revised to

$$Q_{m_i}(\boldsymbol{\rho}_\mathrm{s}, \phi) \equiv \mathrm{i}\rho_0 c_0 k_i \iint_S q_i(\boldsymbol{\rho}_\mathrm{s}, \boldsymbol{\rho}') \phi_{m_i}^*(\boldsymbol{\rho}') \mathrm{d}^2\boldsymbol{\rho}'. \tag{15}$$

2.3 Audio sound field

The source density for audio sound in a 2D rectangular room is obtained by substituting Eq. (12) into Eq. (2)

$$q_\mathrm{a}(\boldsymbol{\rho}_\mathrm{v}) = \frac{\beta k_\mathrm{a}}{\mathrm{i}\rho_0^2 c_0^3} \sum_{m_1, m_2=-\infty}^{\infty} \frac{Q_{m_1}^*(\boldsymbol{\rho}_\mathrm{s}, \psi) Q_{m_2}(\boldsymbol{\rho}_\mathrm{s}, \psi) \phi_{m_1}^*(\boldsymbol{\rho}_\mathrm{v}) \phi_{m_2}(\boldsymbol{\rho}_\mathrm{v})}{S^2(k_1^2 - k_{m_1}^2 + \mathrm{i}k_1 D_{m_1})^*(k_2^2 - k_{m_2}^2 + \mathrm{i}k_2 D_{m_2})}. \tag{16}$$

The audio sound pressure can be expanded similar to the modal expansion given by Eq. (14)

$$p_\mathrm{a}(\boldsymbol{\rho}) = \sum_{m_\mathrm{a}=-\infty}^{\infty} \frac{\psi_{m_\mathrm{a}}(\boldsymbol{\rho}) Q_{m_\mathrm{a}}(\boldsymbol{\rho}_\mathrm{s}, \phi)}{S(k_\mathrm{a}^2 - k_{m_\mathrm{a}}^2 + \mathrm{i}k_\mathrm{a} D_{m_\mathrm{a}})} \tag{17}$$

where $\psi_{m_\mathrm{a}}(\boldsymbol{\rho})$ has the same form given by Eq. (7), m_a denotes the index set of $m_{\mathrm{a},x}$ and $m_{\mathrm{a},y}$, $k_{m_{\mathrm{a},x}} = m_{\mathrm{a},x}\pi/L_x$, $k_{m_{\mathrm{a},y}} = m_{\mathrm{a},y}\pi/L_y$, $k_{m_\mathrm{a}}^2 = k_{m_{\mathrm{a},x}}^2 + k_{m_{\mathrm{a},y}}^2$, and the source term for the audio sound is obtained by Eq. (15)

$$Q_{m_\mathrm{a}}(\boldsymbol{\rho}_\mathrm{s}, \phi) = \mathrm{i}\rho_0 c_0 k_\mathrm{a} \iint_S q_\mathrm{a}(\boldsymbol{\rho}_\mathrm{v}) \phi_{m_\mathrm{a}}^*(\boldsymbol{\rho}_\mathrm{v}) \mathrm{d}^2\boldsymbol{\rho}_\mathrm{v}. \tag{18}$$

Substituting Eq. (16) into Eq. (18) yields

$$Q_{m_\mathrm{a}}(\boldsymbol{\rho}_\mathrm{s}, \phi) = \frac{\beta k_\mathrm{a}^2}{\rho_0 c_0^2} \sum_{m_1, m_2 = -\infty}^{\infty} \frac{Q_{m_1}^*(\boldsymbol{\rho}_\mathrm{s}, \psi) Q_{m_2}(\boldsymbol{\rho}_\mathrm{s}, \psi) I(m_1, m_2, m_\mathrm{a})}{S(k_1^2 - k_{m_1}^2 + \mathrm{i}k_1 D_{m_1})^* (k_2^2 - k_{m_2}^2 + \mathrm{i}k_2 D_{m_2})} \tag{19}$$

where the integral can be calculated analytically

$$I(m_1, m_2, m_\mathrm{a}) \equiv \frac{1}{S} \iint_S \phi_{m_1}^*(\boldsymbol{\rho}_\mathrm{v}) \phi_{m_2}(\boldsymbol{\rho}_\mathrm{v}) \phi_{m_\mathrm{a}}^*(\boldsymbol{\rho}_\mathrm{v}) \mathrm{d}^2\boldsymbol{\rho}_\mathrm{v} = \delta_{m_2, m_1 + m_\mathrm{a}} \tag{20}$$

with the Kronecker delta function $\delta_{m,n} = 1$ when $m = n$ and $\delta_{m,n} = 0$ otherwise. Then Eq. (19) reduces to

$$Q_{m_\mathrm{a}}(\boldsymbol{\rho}_\mathrm{s}, \phi) = \frac{\beta k_\mathrm{a}^2}{\rho_0 c_0^2} \sum_{m_1 = -\infty}^{\infty} \frac{Q_{m_1}^*(\boldsymbol{\rho}_\mathrm{s}, \psi) Q_{m_2}(\boldsymbol{\rho}_\mathrm{s}, \psi)}{S(k_1^2 - k_{m_1}^2 + \mathrm{i}k_1 D_{m_1})^* (k_2^2 - k_{m_2}^2 + \mathrm{i}k_2 D_{m_2})} \tag{21}$$

with $m_{2,x} = m_{1,x} + m_{\mathrm{a},x}$ and $m_{2,y} = m_{1,y} + m_{\mathrm{a},y}$.

Equation (17) is the main result of this paper, which represents the audio sound pressure generated by a PAL in a 2D rectangular room. In Eq.(17), the eigenfunctions $\psi_{m_\mathrm{a}}(\boldsymbol{\rho})$ is obtained by Eq. (7), and the source term $Q_{m_\mathrm{a}}(\boldsymbol{\rho}_\mathrm{s}, \phi)$ is calculated by Eq. (21). The substitution of Eqs. (17), (6), and (11) into Eq. (4) yields the more accurate predictions of the audio sound pressure containing the local effects,

2.4 Source term

To obtain the sound field, the source term for the ultrasound given by Eq. (10) is required to calculate. Many literatures have given the explicit form of the source term for a point source (14), but paid little attention for a line source as shown in Fig. 1, so it will be derived in this subsection. The source density of the line source can be presented under the primed coordinates $O'x'y'$ as

$$q_i(\boldsymbol{\rho}_\mathrm{s}, \boldsymbol{\rho}') = \frac{Q_0}{2a} \Pi\left(\frac{x'}{2a}\right) \delta(y') \tag{22}$$

where Q_0 is a constant with the unit of m^2/s, the denominator $2a$ is to ensure the line source has a total surface velocity of Q_0, $\delta(y')$ is the Dirac delta function, the rectangle function $\Pi(\zeta) = 1$ when $-1/2 < \zeta < 1/2$, and $\Pi(\zeta) = 0$ otherwise.

The primed axes $x'y'$ in Fig. 1 can be seen as rotating the unprimed axes xy counterclockwise through an angle $\vartheta_\mathrm{s} = \mathrm{atan2}(n_{\mathrm{s},x}, n_{\mathrm{s},y})$ followed by a translation of $\boldsymbol{\rho}_\mathrm{s}$. Therefore, the coordinates of a point in the primed system $\boldsymbol{\rho}' = (x', y')$ can be represented by the coordinates in the unprimed one $\boldsymbol{\rho} = (x, y)$ by

$$\boldsymbol{\rho}' = \mathbf{R}(\vartheta_\mathrm{s})(\boldsymbol{\rho} - \boldsymbol{\rho}_\mathrm{s}) \tag{23}$$

where the elementary rotation matrix is

$$\mathbf{R}(\vartheta_\mathrm{s}) = \begin{bmatrix} \cos\vartheta_\mathrm{s} & -\sin\vartheta_\mathrm{s} \\ \sin\vartheta_\mathrm{s} & \cos\vartheta_\mathrm{s} \end{bmatrix}. \tag{24}$$

The substitution of Eq. (24) into Eq. (23) yields the explicit relations

$$\begin{cases} x = x'\cos\vartheta_\mathrm{s} + y'\sin\vartheta_\mathrm{s} + x_\mathrm{s} \\ y = -x'\sin\vartheta_\mathrm{s} + y'\cos\vartheta_\mathrm{s} + y_\mathrm{s}. \end{cases} \tag{25}$$

The source term is then calculated by substituting Eq. (25) into Eq. (10)

$$\begin{aligned} Q_{m_i}(\boldsymbol{\rho}_\mathrm{s}, \psi) = \frac{\mathrm{i}\rho_0 c_0 k_i Q_0}{2a} \int_{0^-}^{0^+} \int_{-a}^{a} & \cos\left[k_{m_{i,x}}(x'\cos\vartheta_\mathrm{s} + y'\sin\vartheta_\mathrm{s} + x_\mathrm{s})\right] \\ & \times \cos\left[k_{m_{i,y}}(-x'\sin\vartheta_\mathrm{s} + y'\cos\vartheta_\mathrm{s} + y_\mathrm{s})\right] \delta(y')\mathrm{d}x'\mathrm{d}y' \end{aligned} \tag{26}$$

which has a closed form with some straightforward derivations

$$Q_{m_i}(\boldsymbol{\rho}_\mathrm{s},\psi) = \frac{\mathrm{i}\rho_0 c_0 k_i Q_0}{2}\Big\{\cos\big(k_{m_{i,x}}x_\mathrm{s}+k_{m_{i,y}}y_\mathrm{s}\big)\,\mathrm{sinc}\left[(k_{m_{i,x}}\cos\vartheta_\mathrm{s}-k_{m_{i,y}}\sin\vartheta_\mathrm{s})a\right] + \cos\big(k_{m_{i,x}}x_\mathrm{s}-k_{m,y}y_\mathrm{s}\big)\,\mathrm{sinc}\left[(k_{m_{i,x}}\cos\vartheta_\mathrm{s}+k_{m_{i,y}}\sin\vartheta_\mathrm{s})a\right]\Big\} \tag{27}$$

where $\mathrm{sinc}(\zeta)\equiv\sin(\zeta)/\zeta$ is the sinc function. For a special case with $\mathbf{n}_\mathrm{s}=(0,1)$, Eq. (27) reduces to

$$Q_{m_i}(\boldsymbol{\rho}_\mathrm{s},\psi) = \mathrm{i}\rho_0 c_0 k_i Q_0\,\mathrm{sinc}(k_{m_{i,x}}a)\,\psi_{m_i}(\boldsymbol{\rho}_\mathrm{s}). \tag{28}$$

3 Simulations

In the following simulations, the average ultrasound frequency $f_\mathrm{u}=(f_1+f_2)/2$ is set to 40 kHz. The audio sound frequency is set to $f_\mathrm{a}=1$ kHz. The sound attenuation coefficients due to the atmospheric absorption are calculated according to ISO 9613 with a temperature of 20°C and a relative humidity of 70% (15). The half-width of the source is set to $a=5$ cm. The surface velocity amplitude is set to $Q_0=0.01\,\mathrm{m}^2/\mathrm{s}$ and $Q_0=2\times10^{-5}\,\mathrm{m}^2/\mathrm{s}$ for the PAL and the conventional dynamic loudspeaker, respectively. The dimensions of the room are $L_x\times L_y=\mathrm{e}/\pi\times1\,\mathrm{m}^2$. The sound field generated by a PAL in free field is obtained using the cylindrical wave expansion method (13). The normalized specific acoustic admittance is set to a constant $\chi(\boldsymbol{\rho})=0.01$ at all frequencies.

Figure 2 compares the linear sound field generated by a line source in free field and in the 2D rectangular room, where Fig. 2(c) represents the audio sound field generated by a conventional dynamic loudspeaker in a room. It is clear that the ultrasound waves at 40 kHz are highly directional in free field, since the aperture size (5 cm) is much larger than the ultrasound wavelength (8.6 mm). In the rectangular room, it is shown in Fig. 2(b) that the major energy of the ultrasound waves is still focused around the radiation axis $x=L_x/2$. This is because the side length in the x direction, L_x, is much larger than the ultrasound wavelength, so that the walls at $x=0$ and $x=L_x$ have little effects. However, many local peaks and valleys are presented in the sound pressure level (SPL) in the y direction, which is resulted from the multiple reflections of the walls at $y=0$ and $y=L_y$. At the audio frequency of 1 kHz, it can be observed in Fig. 2(c) that there are fluctuations and no directional beams are presented.

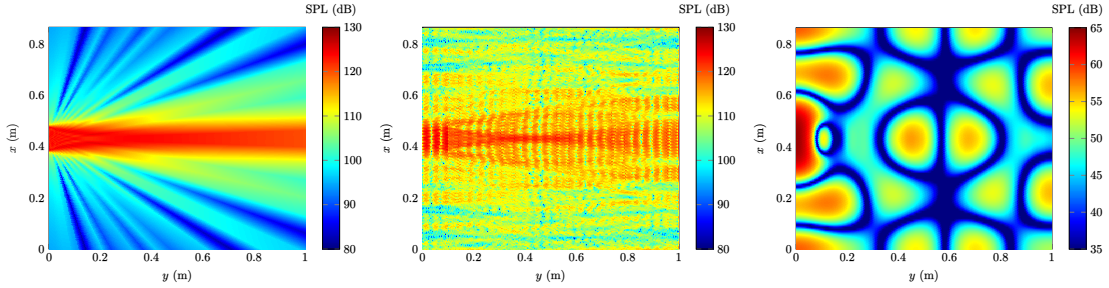

Figure 2. (a) Sound field at 40 kHz in free field with the source centroid at $\boldsymbol{\rho}_\mathrm{s}=(L_x/2,0)$. Sound field at (b) 40 kHz and (c) 1 kHz in the rectangular room with the source centroid at $\boldsymbol{\rho}_\mathrm{s}=(L_x/2,0.1\,\mathrm{m})$.

Figure 3 compares the audio sound field at 1 kHz generated by a PAL in free field and in the rectangular room. As expected, the audio sound field is highly directional in free field even the aperture size (5 cm) is much smaller than the audio wavelength (34.3 cm). In the rectangular room, it is found in Fig. 3(e) that the audio sound appears to be still directional despite some fluctuations in the y axis direction. The distance between adjacent peaks (or valleys) is found to be around half wavelength of the audio sound (17.15 cm). By comparing to the sound of a conventional loudspeaker in a room as shown in Fig. 2(c), it is clear that the advantage of generating directional audio beams is retained for a PAL in a room. It is also found in the top row of Fig. 3 that the SPL difference with and without local effects is negligible except at some locations close to the PAL. This is the reason why most literatures use the Westervelt equation to model the PAL in free field, which is simpler but does not include the local effects (6, 12). However, the SPL difference is significant in the full field when the PAL is placed in a rectangular room as shown in Fig. 3(f). This means the local effects cannot be neglected when modelling the PAL in an enclosure, so the following results are presented with local effects.

Figure 4 shows the sound field generated by a PAL and a conventional loudspeaker when the source centroid is moved close to the left corner of the room. It is observed in Fig. 4(a) that the major part of

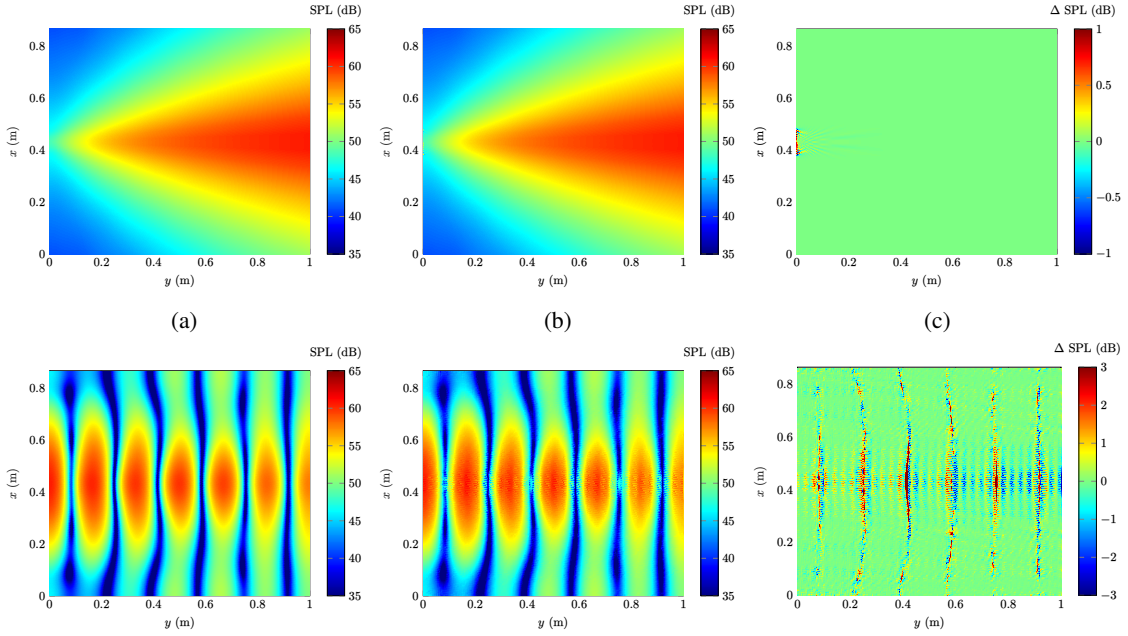

Figure 3. Audio SPL generated by a PAL at 1 kHz. Top row, in free field and $\boldsymbol{\rho}_s = (L_x/2, 0)$; bottom row, in a rectangular room and $\boldsymbol{\rho}_s = (L_x/2, 0.1\,\mathrm{m})$; left column, without local effects; middle column, with local effects; right colulmn, SPL difference with and without local effects.

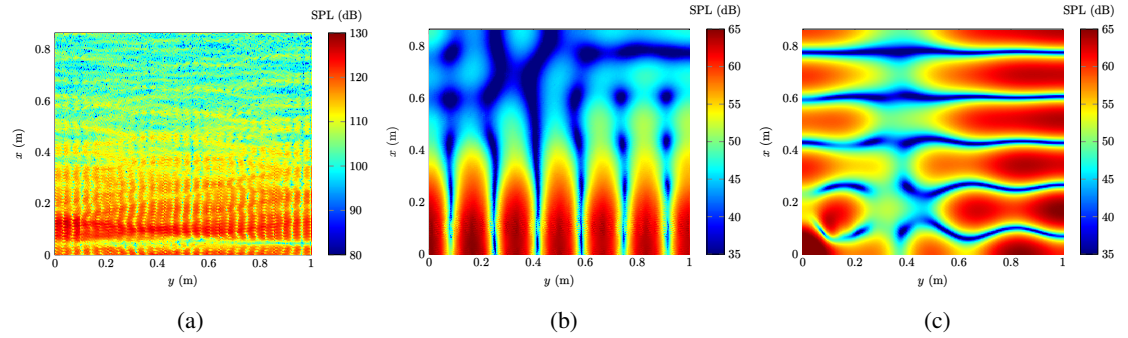

Figure 4. (a) Ultrasound field at 40 kHz and (b) audio sound field at 1 kHz generated by a PAL in a room. (c) Audio sound field at 1 kHz generated by a conventional loudspeaker in a room. The line source centroid is located at $\boldsymbol{\rho}_s = (0.1\,\mathrm{m}, 0.1\,\mathrm{m})$ and the radiation direction $\mathbf{n}_s = (0, 1)$.

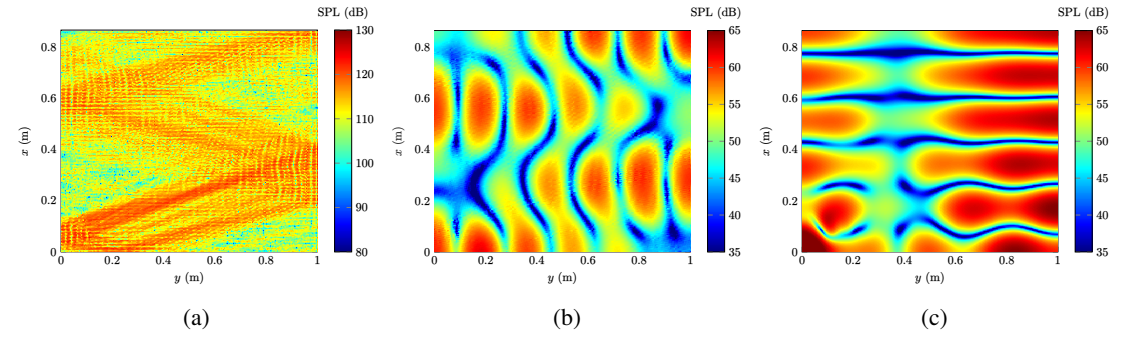

Figure 5. (a) Ultrasound field at 40 kHz and (b) audio sound field at 1 kHz generated by a PAL in a room. (c) Audio sound field at 1 kHz generated by a conventional loudspeaker in a room. The line source centroid is located at $\boldsymbol{\rho}_s = (0.1\,\mathrm{m}, 0.1\,\mathrm{m})$ and the radiation direction is $\mathbf{n}_s = (0.3, 1)$.

ultrasound waves is located below $x = L_x/2$. By comparing Fig. 4(b) to Fig. 3(e), it is clear that audio sound beam is focused on the radiation direction and the SPL is relatively low above $x = L_x/2$. However, the audio sound field generated by a conventional loudspeaker as shown in Fig. 4(c) does not present any directional beams in the radiation direction.

Figure 5 shows the sound field generated by a PAL and a conventional loudspeaker when the line source is not perpendicular to the walls. It can be observed in Fig. 5(a) that the ultrasound waves propagate roughly along the radiation axis and reflect after impinging the walls. Consequently, the audio sound field presented in Fig. 5(b) appears to be still directional in the radiation direction, but with some fluctuations in space. However, the audio sound generated by a conventional loudspeaker shown in Fig. 5(c) is similar to that shown in Fig. 4(c) indicating that the sound field is insensitive to the radiation direction. It is clear that the room has large effects on the radiation of PAL, but in a different way with that on conventional loudspeakers.

4 CONCLUSIONS

An analytical model is developed in this paper to obtain the audio sound field generated by a PAL in a 2D rectangular room with lightly damped walls based on the quasilinear solution and the normal mode expansion. The PAL is modelled by a line source with a finite length and the numerical results are presented and discussed. The results show that the nonlinear local effects are significant in the room which is only observed in the near field when a PAL is placed in free field. This means the nonlinear local effects must be taken into account when modelling the sound generated by a PAL in a room. The simulation results also show that the audio sound field generated by a PAL is still directional in a room. However, the sound pressure level experiences fluctuations along the propagation direction due to the multiple reflections between walls. The model and results presented in this paper bring new insights for the audio applications of using PALs in a room. Although the audio sound is solved in a 2D rectangular room in this paper, the theory can be readily extended for the three-dimensional case which will be investigated in future.

REFERENCES

[1] Gan WS, Yang J, Kamakura T. A Review of Parametric Acoustic Array in Air. Appl Acoust. 2012;73(12):1211-9.

[2] Zhong J, Zhuang T, Kirby R, Karimi M, Zou H, Qiu X. Quiet Zone Generation in an Acoustic Free Field Using Multiple Parametric Array Loudspeakers. J Acoust Soc Am. 2022;151(2):1235-45.

[3] Shi C, Bai R, Gou J, Liang J. Multi-Beam Design Method for a Steerable Parametric Array Loudspeaker. In: 2020 Asia-Pacific Signal and Information Processing Association Annual Summit and Conference (APSIPA ASC); 2020. p. 416-20.

[4] Wang H, Tang J, Wu Z, Liu Y. A Multi-beam Steerable Parametric Array Loudspeaker for Distinct Audio Content Directing. IEEE Sens J. 2022:1-1.

[5] Červenka M, Bednařík M. A Versatile Computational Approach for the Numerical Modelling of Parametric Acoustic Array. J Acoust Soc Am. 2019;146(4):2163-9.

[6] Zhong J, Kirby R, Qiu X. The near Field, Westervelt Far Field, and Inverse-Law Far Field of the Audio Sound Generated by Parametric Array Loudspeakers. J Acoust Soc Am. 2021;149(3):1524-35.

[7] Ganguly A, Vemuri SHK, Panahi I. Real-Time Remote Cancellation of Multi-Tones in an Extended Acoustic Cavity Using Directional Ultrasonic Loudspeaker. In: IECON 2014 - 40th Annual Conference of the IEEE Industrial Electronics Society; 2014. p. 2445-51.

[8] Ji P, Yang J. An Experimental Investigation about Parameters' Effects on Spurious Sound in Parametric Loudspeaker. Appl Acoust. 2019;148:67-74.

[9] Zhong J, Kirby R, Qiu X. A Spherical Expansion for Audio Sounds Generated by a Circular Parametric Array Loudspeaker. J Acoust Soc Am. 2020;147(5):3502-10.

[10] Shi C, Wang Y, Xiao H, Li H. Extended Convolution Model for Computing the Far-Field Directivity of an Amplitude-Modulated Parametric Loudspeaker. J Phys D Appl Phys. 2022;55(24):244002.

[11] Xu B, Sommerfeldt SD. A Hybrid Modal Analysis for Enclosed Sound Fields. J Acoust Soc Am. 2010;128(5):2857-67.

[12] Červenka M, Bednařík M. An Algebraic Correction for the Westervelt Equation to Account for the Local Nonlinear Effects in Parametric Acoustic Array. J Acoust Soc Am. 2022;151(6):4046-52.

[13] Zhong J, Kirby R, Karimi M, Zou H. A Cylindrical Expansion of the Audio Sound for a Steerable Parametric Array Loudspeaker. J Acoust Soc Am. 2021;150(5):3797-806.

[14] Nelson PA, Curtis ARD, Elliott SJ, Bullmore AJ. The Active Minimization of Harmonic Enclosed Sound Fields, Part I: Theory. J Sound Vib. 1987;117(1):1-13.

[15] ISO 9613-1:1993. Acoustics — Attenuation of Sound during Propagation Outdoors — Part 1: Calculation of the Absorption of Sound by the Atmosphere. Genève: International Organization for Standardization; 1993.